Journal of Petroleum Science and Engineering 208 (2022) 109336

Contents lists available at ScienceDirect

Journal of Petroleum Science and Engineering

journal homepage: www.elsevier.com/locate/petrol

Subsea field layout optimization (part III) --- the location-allocation problem of drilling sites

Haoge Liu [a,*], Tor Berge Gjersvik [a], Audun Faanes [a,b]

[a] Department of Geoscience and Petroleum, Norwegian University of Science and Technology, Norway
[b] Equinor ASA, Norway

ARTICLE INFO

Keywords:
Field layout optimization
Location-allocation
BLP
3D dubins curve

ABSTRACT

This study proposes an efficient method to optimize the subsea field layout with the aim of minimizing the subsea field development cost, based on the two methods introduced in Part I and Part II for solving the well trajectory planning problem and the location-allocation problem, i.e., 3D Dubins Curve method and Binary Linear Programming (BLP) method, respectively. The most complex part in subsea field layout optimization is essentially a location-allocation problem of drilling sites embedded with the well trajectory optimization. The full process of our method is clearly summarized in a flowchart. Abundant case studies with comparison to the existing results demonstrate the optimality and the flexibility of our method to solve practical subsea field layout optimization problems. In the cases studies, we also reveal how different user-defined cost items affect the optimal field layout. Details of implementing our method for a better performance is also discussed. This work is the third of a series of papers which systematically introduce an efficient method for subsea field layout optimization to minimize the development cost.

1. Introduction

Subsea field layout design starts from a set of completion intervals provided by geoscientists and reservoir engineers. To minimize the overall field development cost to reach all these completion intervals, especially given that rig mobilization offshore is quite costly, we need optimize the number of drilling sites, economically determine which intervals should be drilled from a specific drilling site and find the best locations for these drilling sites. In short, we need solve the location-allocation problem of drilling sites with the well trajectory optimization embedded.

When wells are drilled from the same drilling site, they are gathered by a template on the seabed. If there is only one well drilled from a drilling site, this single well is set as a satellite well. The conventional template specification based on the maximum number of connected wells includes 2-slot, 4-slot, and 6-slot. A slot of the template can be left vacant, for example, a 4-slot template can be used to connect only 3 wells. Normally, the subsea equipment cost for one *m*-slot template is less than that for *m* satellite wells. The template specification of more slots is available but rarely used because connecting too many wells together tends to make the increment of the drilling cost exceed the saved cost from fewer drilling sites and subsea facilities.

Research on the related topic dates back to 1970s (Devine and Lesso, 1972; Frair and Devine, 1975), where the well construction cost was simplified as a function only related with horizontal distance. In the following decades, quite a few optimization models emerged with different conditions taken into consideration (Dogru, 1987; Hansen et al., 1992; Garcia-Diaz et al., 1996; Iyer et al., 1998; Goel and Grossmann, 2004; Tavallali et al., 2014; Wang et al., 2019). The scope of the optimization model has already reached so large that recent work (Iyer et al., 1998; Goel and Grossmann, 2004; Tavallali et al., 2014; Wang et al., 2019) started to focus on maximizing net present value (NPV), rather than minimizing development cost. No matter how big the scope is, the problem can be mathematically described as a mix-integer nonlinear problem (MINLP), but normally we can only get a local optimal solution of the MINLP model by heuristic algorithms within affordable time. Practically, engineers always reduce the problem to a mix-integer linear problem (MILP) or a mere integer linear problem (ILP) by giving some good options empirically. However, the reduced MILP/ILP model based on experience cannot guarantee the global optimum, either.

This study provides an efficient global-optimal method to deal with

* Corresponding author.
E-mail address: haoge.liu@ntnu.no (H. Liu).

https://doi.org/10.1016/j.petrol.2021.109336
Received 5 April 2021; Received in revised form 5 July 2021; Accepted 3 August 2021
Available online 8 August 2021

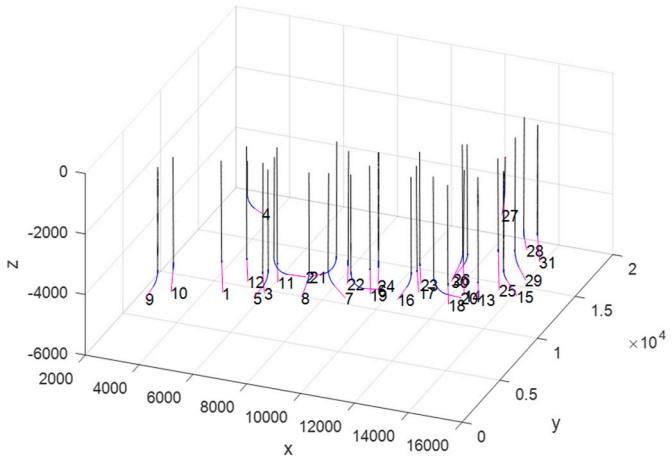

(a) 3D view of satellite wells for dataset 2

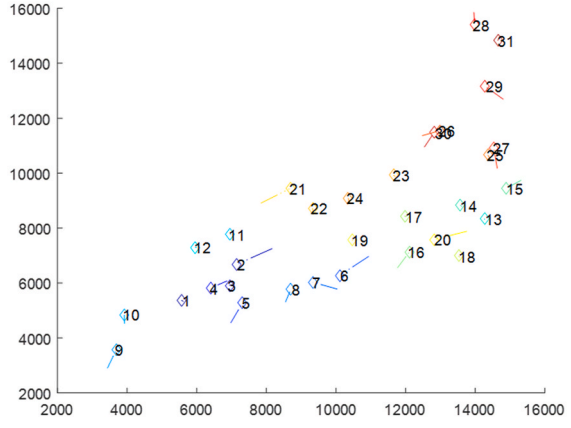

(b) 2D view of satellite wells for dataset 2

Fig. 1. Satellite Wells (dogleg severity = 3°/30 m).

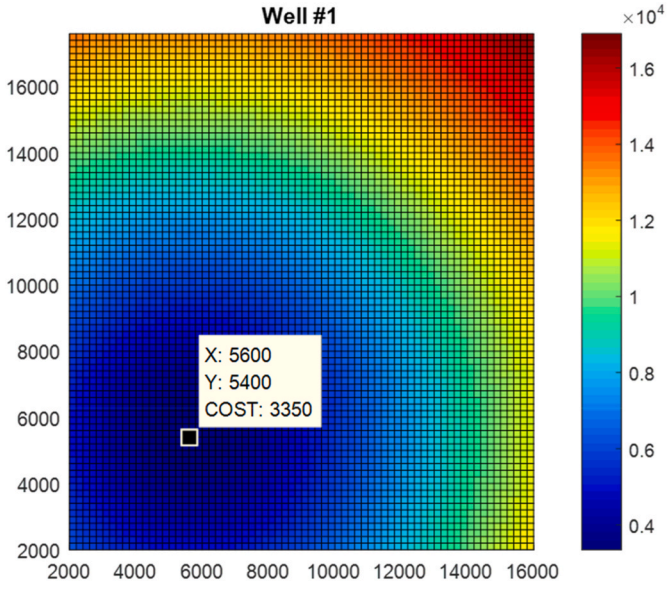

Fig. 2. Optimal cost distribution of well #1.

the location-allocation problem of drilling sites to optimize the subsea field layout with the aim of minimizing the overall field development cost. The problem can be summarized as a "k-sites-n-wells" problem. The method is a systematic combination of the two methods introduced in Part I and Part II: the 3D Dubins Curve for the directional well trajectory planning and the BLP model for the location-allocation problem. The most important feature of our method is that it can provide the global optimal solution of a large-scale problem within a very short time. A brief summary of these two methods is as follows, refer to the Part I and Part II for more details:

(1) The 3D Dubins Curve method provides the optimal trajectory given the positions and drilling directions of a drilling site and a completion point with curvature constraints. More practically, we can use the 3D Dubins Curve method along with the gradient descent method to find the optimal drilling site location common for n ($n \geq 1$) given completion interval(s). Concisely, it solves the "1-site-n-wells" problem, but it cannot handle the "k-sites-n-wells" problem which involves the combinatory problem.

(2) The BLP method can find the global optimal solution to the continuous spaced location-allocation problem with high efficiency, providing the possibility to find the global optimal solution for a more complex problem of a much larger scale. This method was intentionally created by us to solve the location-allocation problem of manifolds, but it also provides the solution to the combinatory problem in the "k-sites-n-wells" problem.

2. Problem description and Basic Assumptions

2.1. Problem description

Given n well completion intervals, $n \in Integer^{+}$, each completion interval is defined by its start point $P_{2,i} = (Px_{2,i}, Py_{2,i}, Pz_{2,i})$ and the end point of the first segment of the completion interval $P_{3,i} = (Px_{3,i}, Py_{3,i}, Pz_{3,i})$, such as the dataset in Appendix II. Thus the drilling direction vector $V_{2,i} = (Vx_{2,i}, Vy_{2,i}, Vz_{2,i})$ is determined, where normally $Vz_{2,i} \leq 0$ so that the direction is not upward. The highest allowed kickoff point $P_{1,i} = (Px_{1,i}, Py_{1,i}, Pz_{1,i})$ for every wellbore should be at the depth of Z_i m, i.e. $Pz_{1,i} = Z_i < 0$, $i \in \{1, 2, \ldots, n\}$. Obviously, the drilling direction vector at every kickoff point is vertical downwards $V_{1,i} = (0, 0, -1)$. The maximum allowed turning rate/dogleg severity is κ°/30 m, i.e. minimum allowed turning rate radius is $r_{\min} = \frac{5400}{\pi\kappa}$ m.

The preparation cost (e.g. rig re-location) for one drilling site is cst_{site}. $cst_{SF,1}$ is the cost of the subsea facilities for a satellite well. Similarly, $cst_{SF,2}$ is for a 2-slot template, $cst_{SF,4}$ is for a 4-slot template, and $cst_{SF,6}$ is for a 6-slot template. The wellbore cost can be a user-defined function related with the trajectory structure following the form as $cst_{Traj} = cstC(Lc) + cstS(Ls,\theta)$, where Lc is the length of non-straight section, Ls is the length of straight section, θ is the inclination angle of the straight section; $cstC(Lc)$ is the cost function of non-straight section which is continuous and positively correlated with Lc, i.e. $\frac{\partial\, cstC(Lc)}{\partial\, Lc} > 0$; $cstS(Ls,\theta)$ is the cost function of straight section which is continuous and positively correlated with Lc and θ, i.e. $\frac{\partial\, cstS(Ls,\theta)}{\partial\, Ls} > 0$ and $\frac{\partial\, cstS(Ls,\theta)}{\partial\, \theta} > 0$.

The objective is to find the optimal combination of these completion intervals so that the overall cost, i.e., the sum of site preparation cost, subsea facility cost and wellbore cost, is minimized. In details, we need determine the allocation relationship between drilling sites and completion intervals; the number of the subsea facilities of different specifications, denoted as $n_{SF,m}$, specifically, $n_{SF,1}$, $n_{SF,2}$, $n_{SF,4}$ and $n_{SF,6}$ are the needed number of subsea facilities for satellite, 2-slot template, 4-slot template and 6-slot template, respectively; the number of the drilling sites n_{site}; and the drilling site location $P_{0,s} = (Px_{0,s}, Py_{0,s}, 0)$, $s \in \{1, 2, \ldots, n_{site}\}$, which is vertically above the corresponding kickoff point (s).

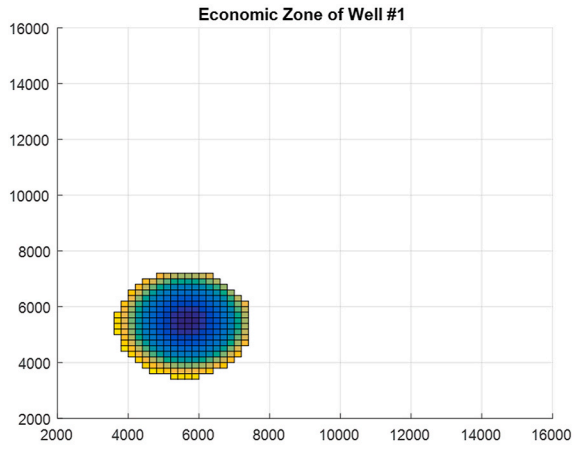

(a) economic zone of well #1

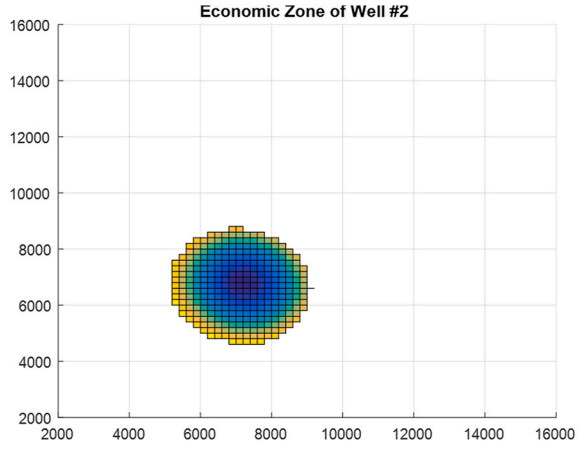

(b) economic zone of well #2

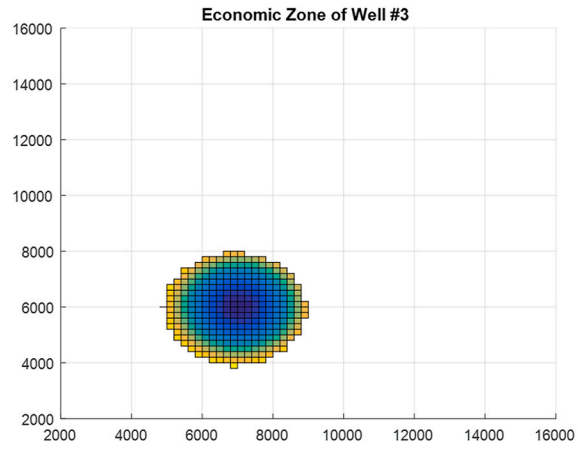

(c) economic zone of well #3

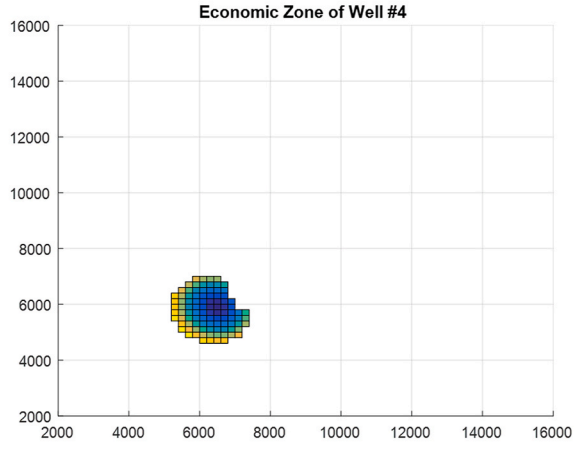

(d) economic zone of well #4

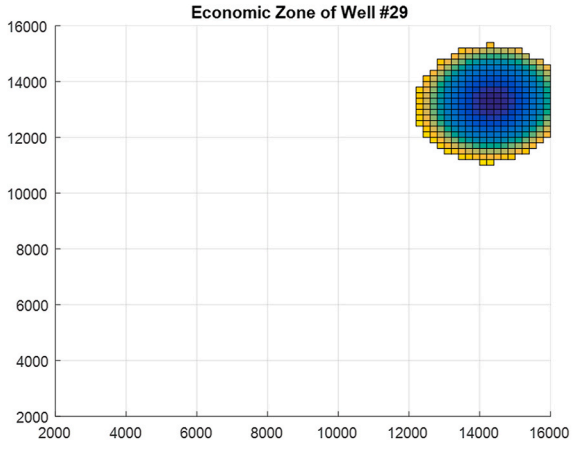

(e) economic zone of well #29

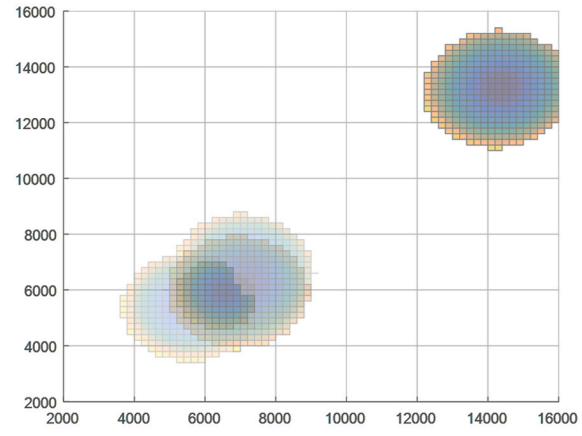

(f) Superposition of Economic Zones of Well #1, #2, #3, #4 and #29

Fig. 3. Example of economic zone ($cst_{site} = 500, cst_{SF1} = 20$).

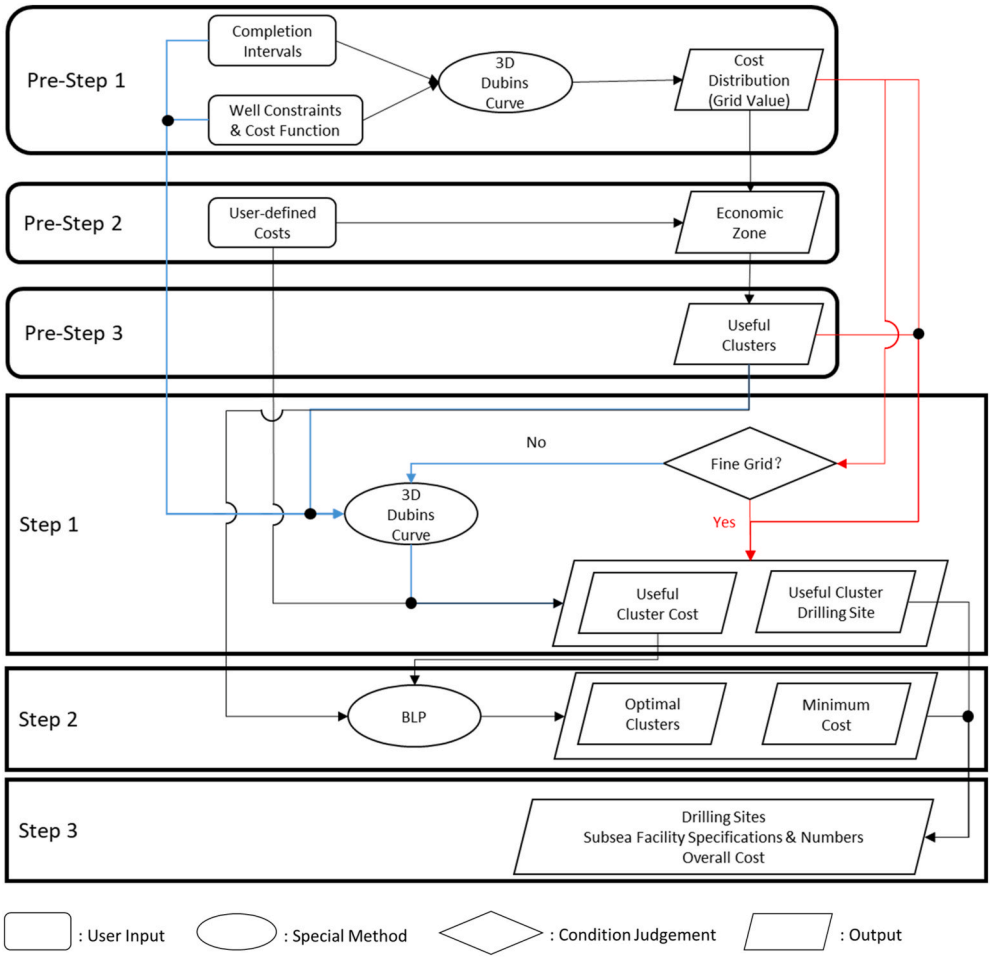

Fig. 4. Flowchart of full process.

Table 1
Result for the layout of satellites only.

Method	User-defined Cost	Layout	$\sum_{j=1}^{N}\gamma_j \cdot cstT_j$	Overall Cost	Total Length of all Wellbores (m)
Lillevik's		Satellite Only			147.95×10^3
Ours	$cst_{site} = 0$ $cst_{SF,1} = 0$ $cst_{SF,2} = 0$ $cst_{SF,4} = 0$ $cst_{SF,6} = 0$	Satellite Only	112180.80	147951.83	147.95×10^3

2.2. Basic Assumption and simplification

1. Fully adopt the assumptions for the 3D Dubins Curve method in Part I.
2. The sea level is $z = 0$. The water depth is assumed to be invariant and shallower than the kickoff point.

3. Methodology

3.1. Mathematical model and main process

This optimization problem can be written as Equation (1). The unknown variables that need to be optimized in the model include the number of drilling sites n_{site}, the number of subsea facilities of different specifications n_{SF}, and the positions P_0 of the n_{site} drilling sites.

$$\begin{aligned} Obj. \quad & \min_{n_{site},n_{SF},P_0} [COST(P_1, V_1, P_2, V_2, r, n_{site}, n_{SF}, cst_{site}, cst_{SF})] \\ & = \min_{n_{site},n_{SF},P_0} \left[n_{site} cst_{site} + \sum_{j=\{1,2,4,6\}} n_{SF,m} cst_{SF,m} + \sum_{i=1}^{n} cst_{Traj,i} \right] \\ s.t. \quad & r \geq r_{\min} \\ & Traj \in Dubins\ Curve \\ & Pz_1 = Z \\ & n_{site} = \sum_{m=\{1,2,4,6\}} n_{SF,m} \end{aligned} \tag{1}$$

This problem can be decomposed into two problems: the optimal

Table 2
Result for the layout of satellites and 2-slot mixed.

Method	User-defined Cost	Layout	$\sum_{j=1}^{N}\gamma_j \cdot cstT_j$	Overall Cost	Total Length of all Wellbores (m)
Lillevik's [10]		{2,5} {3,11} {4,12} {6,8} {7,19} {13,20} {14,18} {15,27} {21,22} {24,30} {25,31} {26,28}; {1} {9} {10} {16} {17} {23} {29}			155.99×10^3
Ours (Case 2.1)	$cst_{site} = 300$ $cst_{SF,1} = 20$ $cst_{SF,2} = 30$	{1,4} {2,11} {3,5} {6,19} {7,8} {9,10} {13,14} {16,17} {18,20} {21,22} {23,24} {25,27} {26,30} {28,31}; {12} {15} {29}	118794.29	154565.32	148.99×10^3
Ours (Case 2.2)	$cst_{site} = 100$ $cst_{SF,1} = 20$ $cst_{SF,2} = 30$	{1,4} {2,11} {3,5} {7,8} {13,14} {16,20} {21,22} {25,27} {26,30} {28,31}; {6} {9} {10} {12} {15} {17} {18} {19} {23} {24} {29}	115286.94	151057.97	148.44×10^3

Table 3
Number of Useful Clusters (satellites and 2-slot mixed).

	Number of Useful Clusters of Size m	
	$m = 2$	$m = 1$
Case 2.1	133	31
Case 2.2	58	

trajectory problem and the location-allocation problem. We have introduced our efficient and global optimal methods for solving these two types of problems in Part I and Part II, respectively. Here we need systematically combine these two methods. Briefly, the main process is as follows:

Step 1. Use the 3D Dubins Curve method to calculate the optimal drilling site $P_{0,j}$ and the related trajectory cost $cst_{Traj,i}$ for each cluster of wells. Here $j \in \left\{1, 2, \ldots, \sum_{m=\{1,2,4,6\}} N_m\right\}$ is the index of clusters of wells; $i \in$ *Cluster* j; N_m is the number of clusters of size m, designated $m \in \{1, 2, 4, 6\}$. The total cost of each cluster $cstT_j$, as Equation (2) shows, includes the cost of all trajectories in the cluster $\sum_{i \in Cluster\ j} cst_{Traj,i}$, the cost of drilling site preparation cst_{site} and the subsea facility cost for the cluster $cst_{SF,m}$, where m is the size of *Cluster* j. For example, if *Cluster* 100 is {5,8,15,20}, it means the *Cluster* 100 is formed by the well #5, #8, #15, and #20, and the cluster size is 4. As we assume water depth to be invariant, the trajectory cost can simply count between the kickoff point and the start point of the completion interval.

$$cstT_j = \left(\sum_{i \in Cluster\ j} cst_{Traj,i}\right) + cst_{site} + cst_{SF,m}, \quad m = \text{size of } Cluster\ j \tag{2}$$

Step 2. Solve the BLP problem shown in Equation (3) to find the best clusters. The summation of N_m is the number of variables in this BLP problem. $\boldsymbol{\gamma}$ Is the variable vector whose dimension is $\sum_{m=\{1,2,4,6\}} N_m \times 1$. $\gamma_j = 1$ means the j cluster is picked for the optimal combination. $\mathbf{A}$ Is the binary coefficient matrix of dimension $n \times \sum_{m=\{1,2,4,6\}} N_m$, $a_{ij} = 1$ means the i completion interval is allocated to the j cluster. If we do not want to use 6-slot templates, we can conveniently set cst_{SF6} a dummy value which is much larger than other subsea facility cost. But the better way is to delete the parameters related 6-slot in Equation (3) so that the computation for irrelevant terms can be avoided.

$$\begin{aligned}
&Obj.\ \min_{\boldsymbol{\gamma} \in Binary} \sum_{j=1}^{N_1+N_2+N_4+N_6} \gamma_j \cdot cstT_j \\
&s.t.\ \ \mathbf{A}_{n \times (N_1+N_2+N_4+N_6)} \boldsymbol{\gamma}_{(N_1+N_2+N_4+N_6) \times 1} = \mathbf{1}_{n \times 1} \\
&\sum_{i=1}^{n} a_{i,j} = 1,\ \forall j = \{1,\ 2, \ldots,\ N_1\} \\
&\sum_{i=1}^{n} a_{i,j} = 2,\ \forall j = \{N_1+1,\ N_1+2, \ldots,\ N_1+N_2\} \\
&\sum_{i=1}^{n} a_{i,j} = 4,\ \forall j = \{N_1+N_2+1,\ N_1+N_2+2, \ldots,\ N_1+N_2+N_4\} \\
&\sum_{i=1}^{n} a_{i,j} = 6,\ \forall j = \left\{\sum_{m=\{1,2,4\}} N_m + 1,\ \sum_{m=\{1,2,4\}} N_m + 2, \ldots,\ \sum_{m=\{1,2,4\}} N_m + N_6\right\} \\
&\mathbf{A} \in Binary
\end{aligned} \tag{3}$$

Table 4
Result for the layout of satellite, 2-slot and 4-slot mixed.

Method	User-defined Cost	Layout	$\sum_{j=1}^{N}\gamma_j \cdot cstT_j$	Overall Cost	Total Length of all Wellbores (m)
Lillevik's [10]		{1,4,11,12} {2,3,5,8} {6,7,22,24} {13,16,17,19} {14,15,18,20} {25,26,27,30}; {9} {10} {21} {23} {28} {29} {31}			157.47×10^3
Ours (Case 3.1)	$cst_{site} = 300$ $cst_{SF,1} = 20$ $cst_{SF,2} = 1e6$ $cst_{SF,4} = 50$	{1,2,3,4} {5,6,7,8} {16,17,18,20} {19,21,22,24} {25,26,27,30}; {9} {10} {11} {12} {13} {14} {15} {23} {28} {29} {31}	119999.13	155770.16	150.50×10^3
Ours (Case 3.2)	$cst_{site} = 300$ $cst_{SF,1} = 20$ $cst_{SF,2} = 30$ $cst_{SF,4} = 50$	{2,3,4,5} {16,17,18,20}; {6,19} {7,8} {9,10} {11,12} {13,14} {21,22} {23,24} {25,27} {26,30} {28,31}; {1} {15} {29}	118542.95	154313.98	149.35×10^3
Ours (Case 3.3)	$cst_{site} = 100$ $cst_{SF,1} = 20$ $cst_{SF,2} = 30$ $cst_{SF,4} = 50$	{1,4} {2,11} {3,5} {7,8} {13,14} {16,20} {21,22} {25,27} {26,30} {28,31}; {6} {9} {10} {12} {15} {17} {18} {19} {23}	115286.94	151057.97	148.44×10^3

Table 5
Number of Useful Clusters (satellites, 2-slot and 4-slot mixed).

	Number of Useful Clusters of Size k		
	$k = 4$	$k = 2$	$k = 1$
Case 3.1	213	133	31
Case 3.2			
Case 3.3	6	58	

$$\mathbf{A}=\begin{bmatrix} a_{1,1} & a_{1,2} & \cdots & a_{1,N_1} & a_{1,N_1+1} & a_{1,N_1+2} & \cdots & a_{1,N_1+N_2} & \cdots & \cdots & a_{1,N_1+N_2+N_4+N_6} \\ a_{2,1} & a_{2,2} & \cdots & a_{2,N_1} & a_{2,N_1+1} & a_{2,N_1+2} & \cdots & a_{2,N_1+N_2} & \cdots & \cdots & a_{2,N_1+N_2+N_4+N_6} \\ \cdot & \cdot & \cdot & \cdot & \cdot & \cdot & \cdot & \cdot & \cdots & \cdots & \cdot \\ \cdot & \cdot & \cdot & \cdot & \cdot & \cdot & \cdot & \cdot & \cdots & \cdots & \cdot \\ \cdot & \cdot & \cdot & \cdot & \cdot & \cdot & \cdot & \cdot & \cdots & \cdots & \cdot \\ a_{n,1} & a_{n,2} & \cdots & a_{n,N_1} & a_{n,N_1+1} & a_{n,N_1+2} & \cdots & a_{n,N_1+N_2} & \cdots & \cdots & a_{n,N_1+N_2+N_4+N_6} \end{bmatrix}$$

Step 3. Count out $n_{SF,m}$ and n_{site} based on the obtained optimal $\boldsymbol{\gamma}$ from Step 2. The objective function of Equation (3) is the same as the objective function of Equation (1). Besides, the drilling sites' positions have already been calculated for all clusters including the optimal ones in Step 1. Hence, Equation (1) is solved.

However, there is a big issue in the process above: if we simply enumerate all the clusters, i.e., $\sum N_m = \sum C_n^m$, the huge number of all possible clusters can easily make the computation in Step 1 infeasible. We need some pre-processing to reduce all the possible clusters to useful clusters.

3.2. Pre-process for reducing possible clusters

In Part II, we introduced Delaunay Triangulation to reduce all possible clusters to only useful clusters by using the adjacency. In this problem the completion interval is not just a point but with a vector. The adjacency we need to find is not within the completion intervals, but within their wellhead locations. However, the wellhead location of a given completion interval is not fixed. We should firstly find the optimal wellhead location for each completion interval individually, then use the Delaunay Triangulation on the wellhead locations. Nevertheless, in this particular type of problems, we have a better way to define the adjacency to limit the useful clusters to a much smaller number.

Pre-Step 1. Assume all the wells to be satellite wells and find the optimal location for each satellite well, as shown in Fig. 1. In Fig. 1(a), the magenta line indicates the completion interval, the black line indicates the straight section, the blue line indicates the curved section. In Fig. 1(b), the diamond shape indicates the satellite wellhead position, the dashed line indicates the curved section of the well, and the different colors indicate different wells.

Meanwhile, we get the optimal cost distribution for each completion intervals within the field by using 3D Dubins Curve method. The optimal cost distribution reveals how the well trajectory cost changes as the satellite drilling site changes. Fig. 2 shows an example of the optimal cost distribution of #1 interval where the trajectory cost is simply defined as the length of the trajectory. The position of minimum cost is the best satellite drilling site. It should be noted that the position/grid resolution of Fig. 2 is only 200 × 200, therefore there is error between the exact minimum value and the minimum value given in the figure. If we set the resolution higher, we can directly use the discretized value in the cost distribution contour to find the optimal drilling site $P_{0,j}$ and total cost $cstT_j$ of each cluster so that we can avoid from conducting the computationally costly 3D Dubins Curve method in the Step 1 of main process. Even though the computational time for pre-process increases if the resolution is set higher, but it is worthwhile to increase the resolution to some extent especially when we are dealing with a large number of wells or with various user-defined cost items.

Pre-Step 2. Set a threshold for the cost distribution of each completion interval to define an economic zone, as shown in Fig. 3. The economic zone is just a clip of the cost distribution contour. The threshold is based on the cost of subsea facilities for a satellite well $cst_{SF,1}$ and the cost of drilling site preparation cst_{site}, as shown in Equation (4). $\min(cst_{Traj,i})$ is the minimum of the cost distribution, such as the data cursor shows in Figs. 2 and 3(a); the corresponding position of $\min(cst_{Traj,i})$ is the best drilling site as a satellite for that #i well interval. The *factor* is used to control the possible numerical error in the discretized grid value so that we will not miss any optimal cluster. However, setting *factor* too large will introduce more useless clusters as useful clusters. We can roughly set it between 1 and 1.2 based on the resolution of the cost distribution. The logic of the threshold Equation (4) is that if the well is drilled as a template well and the drilling site is outside the economic zone, then the

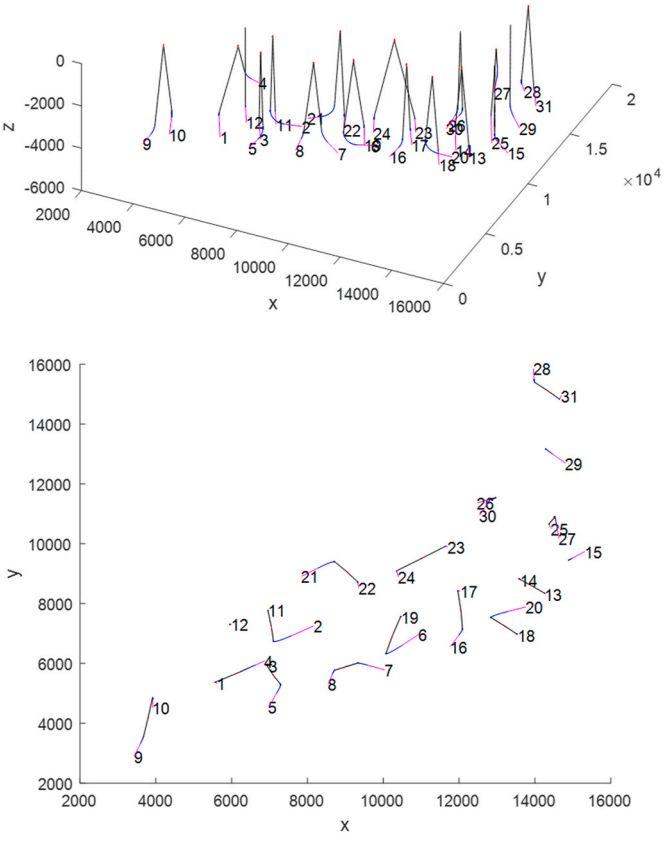

Fig. 5. Optimal layout for case 2.1.

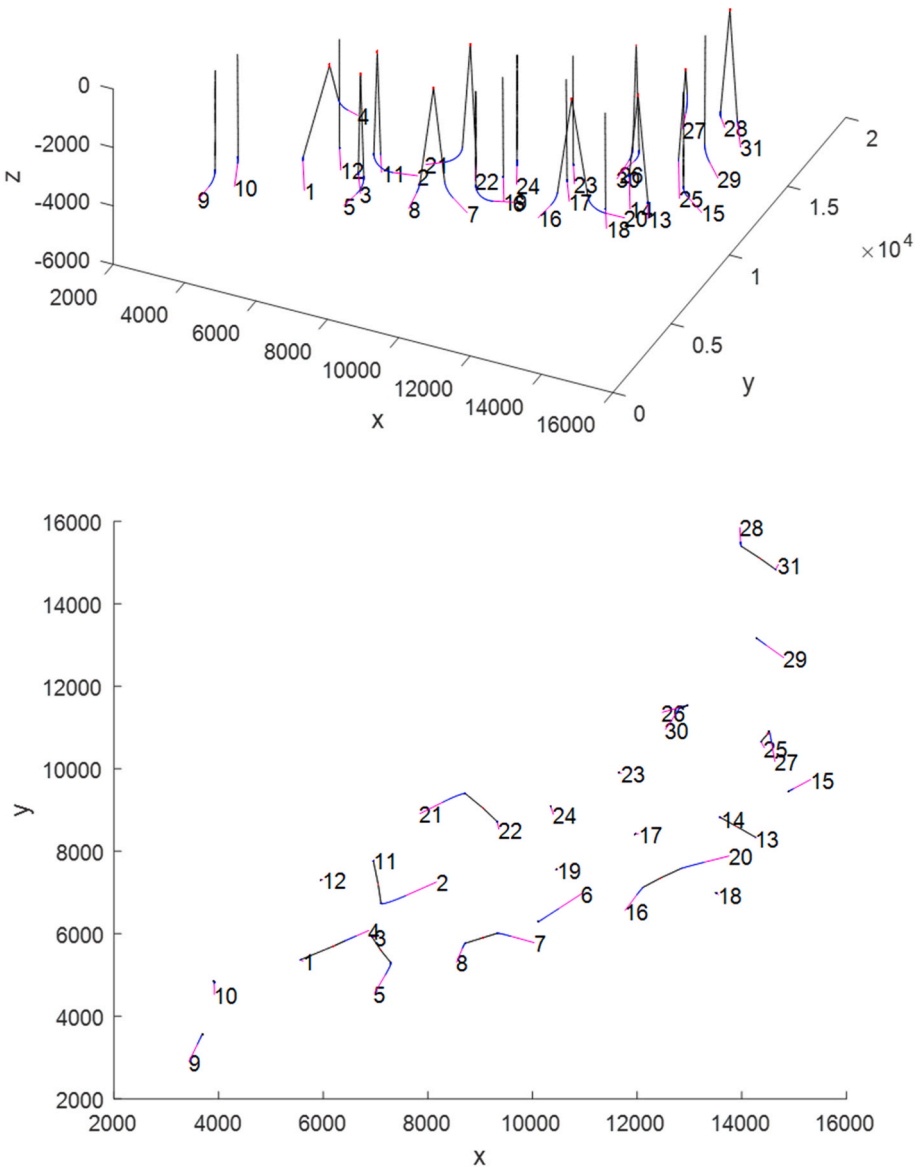

Fig. 6. Optimal layout for case 2.2.

trajectory cost will exceed the saved cost from less drilling sites and less subsea facilities, which means it is better to drill the well as a satellite well rather than a template well. In other words, it is economic only if the template drilling site for the well is within its economic zone. Hence, in the Pre-Step 1 we do not need to compute the cost distribution on the whole field for a given well interval, we just need to compute from the assumed satellite wellhead position to the economic zone boundary.

$$threshold_i = \min\left(cst_{Traj,i}\right) + \left(cst_{site} + cst_{SF,1}\right) \times factor \tag{4}$$

Pre-Step 3. Superpose the economic zones to find the useful clusters. If n wells should be drilled as template wells from one drilling site, then the economic zones of the n wells must have a common overlapped zone. As Fig. 3 shows, wells #1, #2, #3 and #4 have a common overlapped zone around (6000,6000), therefore these four wells can form a useful cluster of size 4 to be drilled as a 4-slot template. Of course, any two of these four wells can form a useful cluster of size 2 to be drilled as a 2-slot template. While well #29 has no overlapped zone with these four wells, therefore, none of these four wells can form a cluster with the well #29. With such a strategy, the number of the useful clusters we need to compute in the main process will be very small.

It should be noted that the economic zone of well #4 shown in Fig. 3 (d) is not as regular as the others, because there is a blank area in its optimal cost distribution, i.e., if the drilling site is located in the blank area, the well completion interval #4 can't be reached. The reason is that the interval #4 is relatively shallow as shown in Fig. 1(a).

3.3. Flowchart of Full Process

A flowchart of the full process is shown in Fig. 4 for a better understanding of our method. It should be noted that the most time-consuming part in the process is the 3D Dubins Curve method in Pre-Step 1 and main Step 1. Hence, we provide two choices for the workflow indicated by red lines and blue lines in the flowchart (see Table 7).

As the red lines indicate, if the grid resolution in Pre-Step 1 is fine enough, we can safely use the information calculated based on the grid values to save some computational time in main Step 1 b y avoiding doing 3D Dubins Curve method to calculate the accurate information of useful clusters; otherwise, as the blue lines indicate, we must use the 3D Dubins Curve method again to refine the information of useful clusters. You may have doubt that the calculation based on grid values will not provide the global optimal solution. Indeed, if the grid is coarse, it may not even provide the optimal layout, as shown in Table 8. But once the

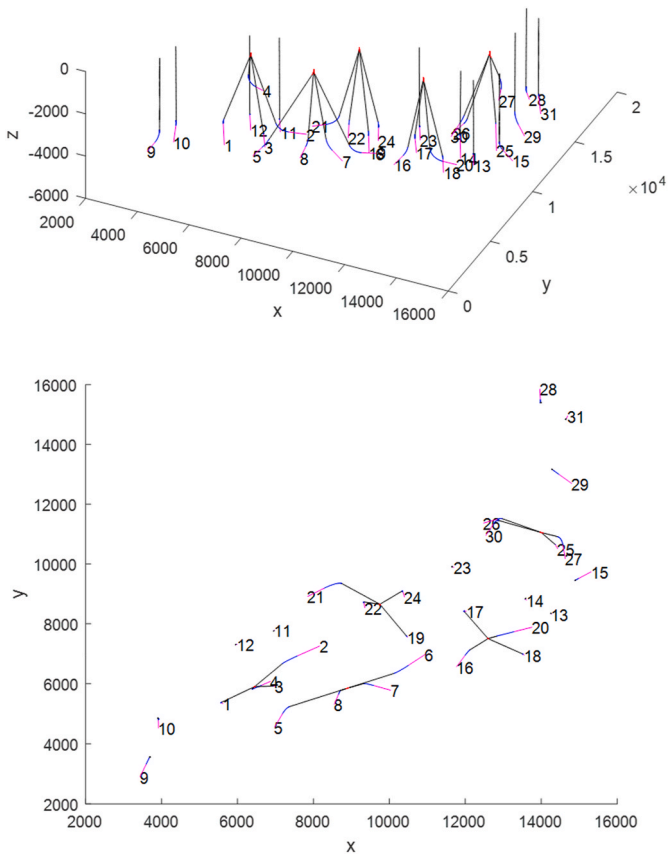

Fig. 7. Optimal layout for case 3.1.

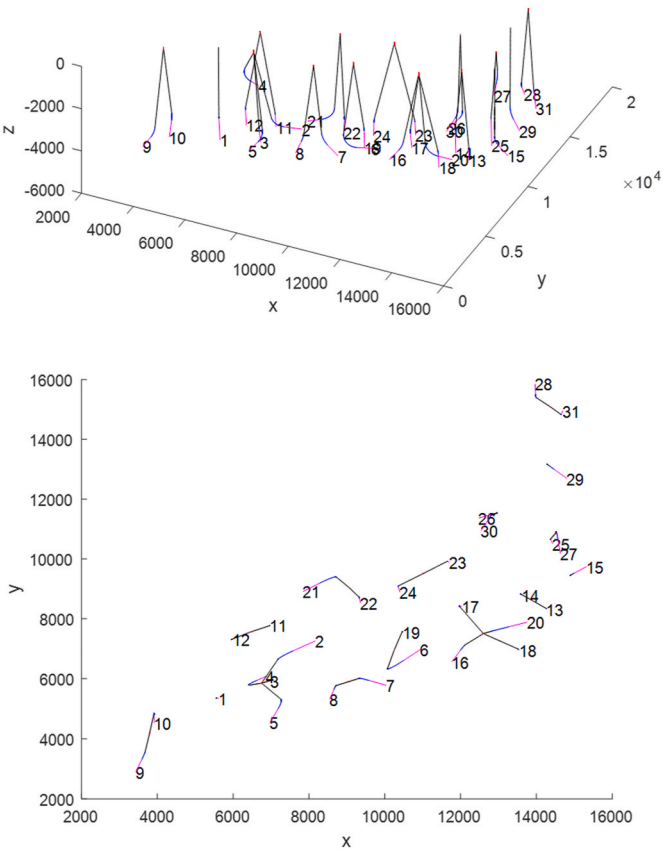

Fig. 8. Optimal layout for case 3.2.

grid is fine, the error becomes small enough to become acceptable, as shown in Table 9. The strategy for the grid resolution is further discussed in Section 5.3.In Step 2, feed the information of useful clusters into the BLP method to find out the optimal clusters and the corresponding minimum cost. With the optimal clusters obtained, we can gather the information with some basic calculations to get the final solution in Step 3 (see Table 6).

4. Case study

The data used in Lillevik's work (Lillevik and Standal, 2018) is given in Appendix II. The Dataset 1 is an intentionally forged dataset where all the completion intervals are horizontal and located at the same depth. The Dataset 2 is real field data. In this Section, we just use the Dataset 2. Dataset 1 will be used for further discussion in the next Section.

For comparison, we fully adopt Lillevik's parameters: depth of kick off point is 500 m, i.e. $Pz_{1,i} = -500$; the maximum allowed turning rate is 3°/30 m. As Lillevik's aim is the minimum total length of all wells, therefore we set the cost function of well trajectory to be the trajectory length, i.e. $cst_{Traj} = cstC(Lc) + cstS(Ls, \theta) = Lc + Ls$. Lillevik's work cannot take other factors into consideration, but ours can involve the site preparation cost and subsea facility cost. Even though the objectives are different, we can still have a comparison on the total length of the wells. As for the other user-defined costs, we will manipulate them in the following cases to see how they affect the optimal field layout.

The cost and the length calculated by our method in the Case Study are all based on the discretized/grid values of the optimal cost distribution, i.e. the output of Pre-Step 1, with the grid resolution of 50 m × 50 m. Beside, set $factor = 1.2$ in Equation (4) for the case study here. The values for user-defined cost are dimensionless corresponding to the length of the wellbore trajectory. Practically, you can simply take in the real cost functions for wellbore trajectories and the real values for cost

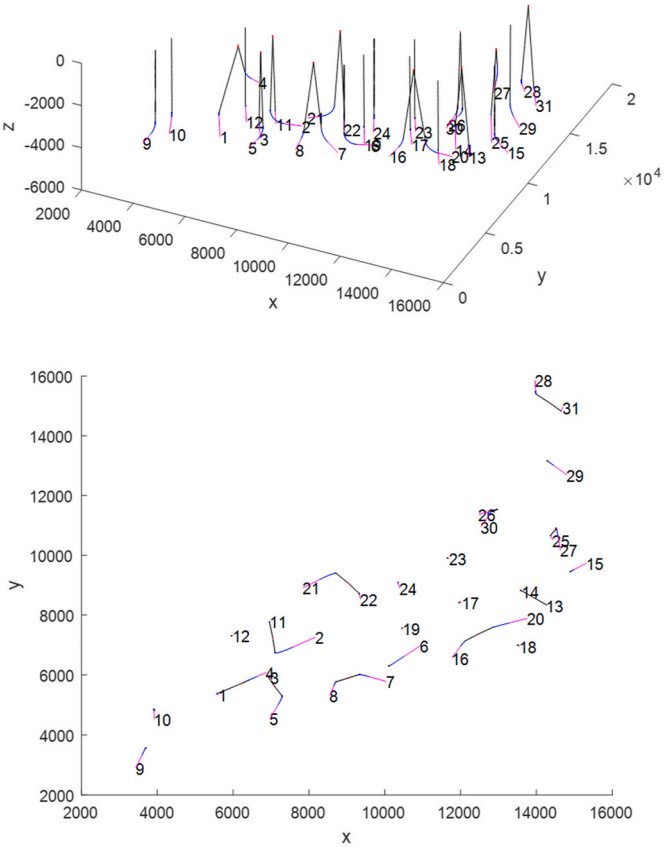

Fig. 9. Optimal layout for case 3.3.

Table 6
Result for the layout of with vacant slot allowed.

	User-defined Cost	Layout	$\sum_{j=1}^{N} \gamma_j \cdot cstT_j$	Overall Cost	Total Length of all Wellbores (m)
Case 4	$cst_{site} = 300$ $cst_{SF,1} = 20$ $cst_{SF,2} = 30$ $cst_{SF,3} = 50$ $cst_{SF,4} = 50$	{1,3,4,5}; {2,11,12} {13,14,15} {16,18,20} {21,22,24}; {6,19} {7,8} {9,10} {17,23} {25,27} {26,30} {28,31}; {29}	118192.40	153963.43	149.58×10^3

Table 7
Number of Useful Clusters (vacant slot allowed).

	Number of Useful Clusters of Size k			
	$k = 4$	$k = 3$	$k = 2$	$k = 1$
Case 4	213	237	133	31

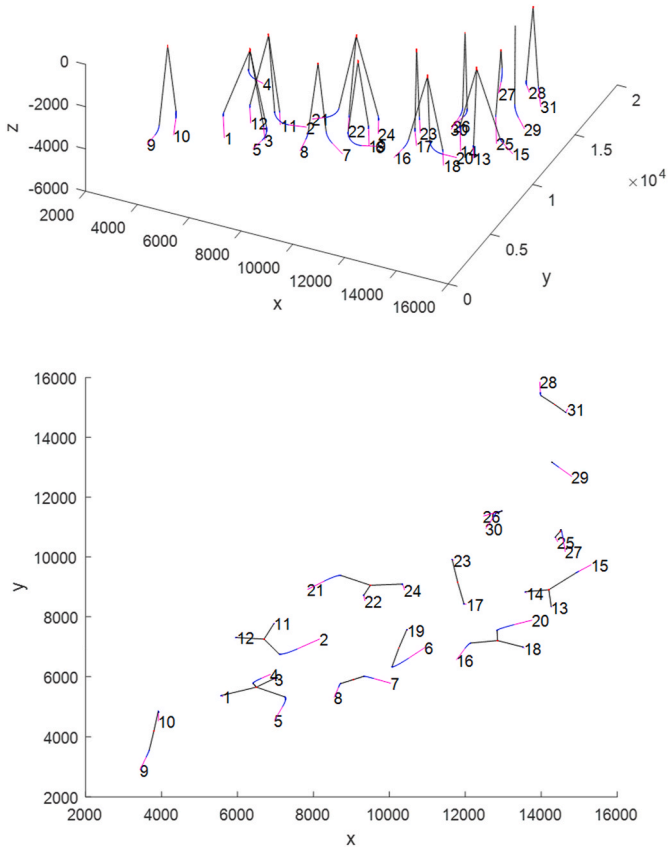

Fig. 10. Optimal layout for case 4.

items.

4.1. Case 1: satellite only

We Intentionally make a case where $cst_{site} = 0$, $cst_{SF,i} = 0, i \in \{1, 2, 4, 6\}$. This case guarantees the optimal layout to be all satellite wells. Because $cst_{site} = 0$ means that we can move the rig and prepare the drilling site arbitrarily without considering the cost; $cst_{SF,i} = 0$ means that the template does not save any money. This case can be a validation for the correctness of our optimization method. Results are shown in Table 1. The drilling site position for each completion interval is shown in Appendix III. Because all the wells are satellite, the accurate value of each site position obtained in Pre-Step 1 is also provided.

$\sum_{j=1}^{N} \gamma_j \cdot cstT_j$ is the result from Equation (3), which counts the total cost from the kickoff point to the start point of completion interval for all wells. The overall cost need add the total cost above the kickoff point for all wells which is 15,500 and the total cost of the completion intervals for all wells is 20,271.03. As we set $cst_{site} = 0$ and $cst_{SF,i} = 0$, the overall cost is just the total length of all wells.

4.2. Case 2: satellite and 2-slot mixed

Now consider there are only satellite wells and 2-slot templates. We simply delete the parameters related with 4-slot and 6-slot in Equation (3). Change the user-defined cost, we will see different optimal layout generated by our method. Results are shown in Table 2. By comparing the total length, we can see that Lillevik's work is just a suboptimal solution. Comparing the optimal layouts of the Cases, it tells that the optimal layout tends to have more satellites if the cost of site preparation is less, which matches with the engineering intuition. Fig. 5 and Fig. 6 show the optimal layout for Case 2.1 and Case 2.2, respectively. The magenta line indicates the completion interval, the black line indicates the straight section, the blue line or the red line indicates the curved section. The drilling site position for each completion interval is shown in Appendix III. The number of useful clusters is shown in Table 3.

It should be noted that, the overall cost includes the site cost and the subsea facility cost which are now not 0, we need deduct the cost of rigs and wellheads from the overall cost to obtain the total length of all wellbores. Take the Case 2.1 for example, the optimal layout tells there are 14 2-slot templates and 3 satellites, incurring the site cost $14 + 3 = 17$ times, hence the difference between the value of overall cost and the value of the total length of all wellbores is $17cst_{site} + 14cst_{SF,2} + 3cst_{SF,1} = 5580$.

4.3. Case 3: satellite, 2-slot and 4-slot mixed

Lillevik's work did not provide the layout with more than 2 types of manifolds. For comparison, we set a dummy value for cst_{WH2} to find the optimal layout of satellite and 4-slot mixed. Change the user-defined cost, we will see different optimal layout generated by our method. Results are shown in Table 4. Fig. 7, Fig. 8 and Fig. 9 show the optimal layout for Case 3.1, Case 3.2, and Case 3.3, respectively. The drilling site position for each completion interval is shown in Appendix III. The number of useful clusters is shown in Table 5 (see Fig. 10).

Table 8
Coarse resolution fails to obtain global optimal layout.

Resolution (m×m)	User-defined Cost	Layout	$\sum_{j=1}^{N}\gamma_j \cdot cstT_j$	Overall Cost	Total Length of all Wellbores (m)
200x200	$cst_{site}=0$ $cst_{SF,1}=0$ $cst_{SF,2}=0$ $cst_{SF,4}=0$ $cst_{SF,6}=0$	{10,13} {11,21}; Satellite for the others	69860.33	112394.39	112394.39
50x50		Satellite only	69814.39	112348.44	112348.44

Table 9
Comparison between grid value and accurate value for Case 3.3

Method	User-defined Cost	Layout	$\sum_{j=1}^{N}\gamma_j \cdot cstT_j$	Overall Cost	Total Length of all Wellbores (m)
Case 3.3 (50x50)	$cst_{site}=100$ $cst_{SF,1}=20$ $cst_{SF,2}=30$ $cst_{SF,4}=50$	{1,4} {2,11} {3,5} {7,8} {13,14} {16,20} {21,22} {25,27} {26,30} {28,31}; {6} {9} {10} {12} {15} {17} {18} {19} {23} {24} {29}	115286.94	151057.97	148437.96
Case 3.3 (200x200 & refinement by 3D Dubins method)		{1,4} {2,11} {3,5} {7,8} {13,14} {16,20} {21,22} {25,27} {26,30} {28,31}; {6} {9} {10} {12} {15} {17} {18} {19} {23} {24} {29}	115284.97	151056.00	148436.00

4.4. Case 4: vacant slot allowed

The cases above have demonstrated the feasibility and advantage of our method, especially comparing to the existing work, and it will be quite meaningless to show more cases of the layout of mixing satellite, 2-slot, 4-slot, 6-slot, etc.

Practically, the *m*-slot template may not be fully occupied, for example, one 4-slot template only connects 3 wells with 1 slot left vacant. To deal with such a scenario, we can simply add the cluster of size 3 into Equation (3) and set $cst_{SF,3} = cst_{SF,4}$. Take the Case 3.2 for comparison, results are shown in Table 6. Compared to the Case 3.2, we can see that with vacant slot allowed, the overall cost is reduced, while the total length of all wellbores is increased. Fig. 10 shows the optimal layout for Case 4. The number of useful clusters is shown in Table 7.

5. Further discussion

5.1. Variable water depth

For simplicity of the Case Study above, we made the Basic Assumption 2 where the water depth is assumed to be constant across the field, resulting in the cost above kickoff point as an invariant once the kickoff depth is fixed. However practically, the depth of the water can change over the lateral extent of the field, resulting in large difference in the cost above kickoff point, where the cost above kickoff point can no longer be treated as an invariant. For such a scenario, the solution is quite easy: modify Equation (2) to let the total cost of a cluster $cstT_j$ includes the cost above the kickoff point of the cluster.

5.2. Involving the cost of flowlines on seabed

If we want to involve the cost of flowlines on seabed into the overall cost, we can firstly use the method introduced in this study to obtain the global optimal layout of wellheads, i.e., the wellheads' positions, which will then be used as the input for the method introduced in Part II to obtain the global optimal for flowlines. This workflow cannot guarantee the global optimal for the overall cost because the cost of flowlines directly depends on the layout of wellheads, but not the layout of completion intervals. Nevertheless, as the cost for wellbores is much higher than the cost for flowlines, we can safely regard the sum of these two correlated global optimal results as an extremely good optimal which is very likely to be the global optimal.

Strictly, to ensure the global optimal, we should enumerate the layouts of wellheads from the minimum cost to a higher cost where the gap between the higher cost and the minimum cost is enough to cover the cost of flowline.

5.3. Strategy for grid resolution

Table 8 shows an example where the coarse resolution cannot obtain global optimal layout: for Dataset 1, set the cost of drilling site preparation and subsea facilities to be 0, then the layout result should be satellites only, just as the Case 1 for Dataset 2. However, the result based on the grid value with the resolution of 200m × 200 m turns out that there are two 2-slot templates in the optimal layout. Improving the resolution is the logical solution, but it takes much longer time for pre-process. For example, the pre-process time for the resolution of 50m × 50 m is 16 times that of the resolution of 200m × 200 m.

Alternatively, we can use the 3D Dubins Curve method to refine the information of useful clusters based on coarse grid values, i.e., to accurately calculate the optimal drilling site $P_{0,j}$ and trajectory cost $cst_{Traj,i}$ for each useful cluster of wells, and then obtain the $cstT_j$. Come back to the real field Dataset 2 and take the Case 3.3 for example. If we set a coarse grid in Pre-Step 1 and then use 3D Dubins Curve method in main Step 1, we will still get the accurate values. The results are shown in Table 9 and Appendix III. We can see that there is no difference in the optimal layout, and the difference in the cost value is so small that we can safely ignore it. The additional computational time for using 3D Dubins Curve in main Step 1 is around 77 s, conducted on an Intel Core i7-10750H CPU. The time of Pre-Step 1 under parallel computation of 4 workers is around 118 s for the resolution of 200m × 200 m and 1776 s for 50m × 50 m.

We can see that for the computation of a single case, it costs less time to use a coarse grid and then use 3D Dubins Curve method in main Step 1. However, do not forget that the result from Pre-Step 1 can be reused for other cases of different user-defined subsea facility costs and site preparation costs. We can imagine that if the coarse grid values cannot be used in main Step 1 and we must refine the information of useful clusters, then after several computations of different cases, the sum of the additional time we spend on main Step 1 in these different cases can easily exceeds the time saved by a coarse resolution for pre-process.

Therefore, the strategy for grid solution is as follows:

1 If every cost function is well defined, practically it means that we have confirmed the facility providers and service providers for the field development, and we just need to find the optimal solution for one case, then we shall use coarse grid in Pre-Step 1, followed by 3D Dubins Curve method in main Step 1.
2 Otherwise, use a moderately fine resolution, but no need to be extremely fine. Then only if we are not satisfied or have doubt in the results based on grid values, use 3D Dubins Curve method in main Step 1 to refine the information of useful clusters.

6. Conclusion

Based on the two methods introduced in Part I and Part II, we build an efficient global-optimal method to deal with the location-allocation problem of drilling sites to optimize the subsea field layout with the aim of minimizing the overall field development cost. A flowchart which clearly shows the full process of our method is created. Case studies show how the cost items affect the optimal layout. The correctness and the flexibility of our method to solve the comprehensive and practical subfield optimization problems are well demonstrated. Besides, the strategy for grid resolution is also discussed. We are confidently expecting that significant amount of money can be saved by the global optimal solution provided by our method in the field development.

CRediT author statement

Haoge Liu, Tor Berge Gjersvik, Audun Faanes

Declaration of competing interest

The authors declare that they have no known competing financial interests or personal relationships that could have appeared to influence the work reported in this paper.

Acknowledgement

This work was carried out as a part of SUBPRO, a Research-based Innovation Centre within Subsea Production and Processing. We gratefully acknowledge the project support from SUBPRO (grant number 237893), which is financed by the Research Council of Norway, major industry partners and NTNU.

Appendix I. List of Symbols

$P_{0,j}$: $(Px_{0,j}, Py_{0,j}, 0)$, the drilling site position for j-th cluster, vertically above the corresponding kickoff point(s);
$P_{1,i}$: $(Px_{1,i}, Py_{1,i}, Pz_{1,i})$, the highest allowed kickoff point for i-th well;
$V_{1,i}$: $(0, 0, -1)$, the drilling direction at $P_{1,i}$;
$P_{2,i}$: $(Px_{2,i}, Py_{2,i}, Pz_{2,i})$, the start point of the i-th completion interval;
$P_{3,i}$: $(Px_{3,i}, Py_{3,i}, Pz_{3,i})$, the end point of the first segment of i-th completion interval;
$V_{2,i}$: $(Vx_{2,i}, Vy_{2,i}, Vz_{2,i})$, the drilling direction at $P_{2,i}$;
κ: the maximum turning rate/dogleg severity, °/30 m;
$r_{\min}$: the minimum turning rate radius, m;
cst_{site}: the preparation cost for one drilling site;
$cst_{SF,m}$: the cost of the subsea facility for a m-slot template; particularly, when $m = 1$, it means satellite well;
n_{site}: the number of drilling site;
$n_{SF,m}$: the number of m-slot subsea facilities.
$cst_{Traj,i}$: the wellbore cost of i-th well;

$cstT_j$: the total cost of j-th cluster;
N_m: the number of clusters of size m;
$\boldsymbol{\gamma}$: the BLP binary variable vector;
Lc: the length of the non-straight/circular section;
Ls: the length of the straight section;
θ: the inclination angle of the straight section;
$cstC(Lc)$: the cost function of the non-straight section;
$cstS(Ls,\theta)$: the cost function of the straight section;

Appendix II. Dataset of Well Completion Intervals

Dataset 1

Well Index	Start Point			End Point		
	x	y	z	x	y	Z
1	286	786	2500	71	1500	2500
2	2714	2786	2500	1786	2143	2500
3	2571	2714	2500	1571	3143	2500
4	1786	4143	2500	500	4714	2500
5	2000	4214	2500	2857	4000	2500
6	2786	4429	2500	3786	4500	2500
7	3000	5071	2500	3714	4714	2500
8	3357	5429	2500	3786	5214	2500
9	3714	3357	2500	4500	3429	2500
10	6786	3571	2500	6571	2857	2500
11	7143	4071	2500	6786	3786	2500
12	7500	4500	2500	6786	5286	2500
13	7500	4071	2500	8714	3929	2500
14	9429	6571	2500	8857	5929	2500
15	9571	4429	2500	10,000	4286	2500
16	11,357	4500	2500	11,929	4143	2500
17	10,214	5214	2500	10,714	5643	2500
18	7857	6286	2500	8857	5821	2500
19	8429	4500	2500	7714	5357	2500
20	9643	3571	2500	9071	2857	2500
21	7714	3786	2500	7857	2857	2500
22	7571	893	2500	7143	571	2500
23	5357	3143	2500	4714	1929	2500
24	4500	4500	2500	5000	5143	2500
25	3357	1143	2500	3000	571	2500
26	1071	1714	2500	1500	2714	2500
27	786	786	2500	500	1571	2500
28	2643	5929	2500	1643	5429	2500
29	5929	2286	2500	6214	1071	2500
30	10,571	3429	2500	11,571	2571	2500

Dataset 2

Well Index	Start Point			End Point		
	x	y	z	x	y	Z
1	5565	5364	3850	5614	5335	4852
2	7578	6922	4368	8166	7252	4451
3	6939	5918	4179	6997	5920	4801
4	6630	5944	2066	6869	6075	2235
5	7188	5004	4311	6978	4553	4567
6	10,500	6606	4284	10,939	6969	4352
7	9586	5938	4143	10,034	5781	4438
8	8661	5646	4117	8550	5311	4536
9	3595	3324	4409	3434	2902	4698
10	3918	4803	4219	3921	4524	4870
11	6960	7764	4361	6976	7785	4962
12	5957	7304	4234	5993	7303	4965
13	14,262	8338	3992	14,268	8316	4512
14	13,577	8829	3527	13,614	8788	4614
15	14,984	9513	4086	15,315	9737	4640
16	11,993	6938	4114	11,769	6560	4434
17	11,972	8424	4009	12,029	8426	4667
18	13,520	6981	3800	13,554	6945	4422
19	10,463	7570	3939	10,484	7545	4737
20	13,283	7731	4355	13,757	7882	4434

(*continued on next page*)

(*continued*)

Well Index	Start Point			End Point		
	x	y	z	x	y	Z
21	8287	9189	4858	7848	8910	4949
22	9330	8699	4299	9357	8534	4848
23	11,658	9918	4265	11,700	9881	4855
24	10,356	9062	4278	10,400	8892	4825
25	14,367	10,650	3584	14,434	10,507	4795
26	12,852	11,499	4474	12,480	11,367	4967
27	14,568	10,649	1901	14,632	10,176	2195
28	13,977	15,499	4540	13,963	15,852	5030
29	14,467	12,996	4712	14,803	12,691	5011
30	12,748	11,346	4424	12,541	10,953	4929
31	14,652	14,836	4163	14,696	14,954	5054

Appendix III. Drilling Site Positions for Case Study (Grid Value)

Case 1

Well Index	Drilling Site Position		Difference
	Grid Value	Accurate Value	
1	(5550; 5350;-500)	(5564; 5364;-500)	(14; 14; 0)
2	(7150; 6700;-500)	(7139; 6676;-500)	(-11;-24; 0)
3	(6950; 5900;-500)	(6937; 5918;-500)	(-13; 18; 0)
4	(6400; 5800;-500)	(6392; 5814;-500)	(-8; 14; 0)
5	(7300; 5300;-500)	(7319; 5286;-500)	(19;-14; 0)
6	(10,100; 6300;-500)	(10,111; 6284;-500)	(11;-16; 0)
7	(9350; 6050;-500)	(9331; 6028;-500)	(-19;-22; 0)
8	(8700; 5750;-500)	(8703; 5774;-500)	(3; 24; 0)
9	(3700; 3550;-500)	(3689; 3571;-500)	(-11; 21; 0)
10	(3900; 4850;-500)	(3917; 4849;-500)	(17;-1; 0)
11	(6950; 7750;-500)	(6960; 7764;-500)	(10; 14; 0)
12	(5950; 7300;-500)	(5956; 7304;-500)	(6; 4;0)
13	(14,250; 8350;-500)	(14,262; 8339;-500)	(12;-11; 0)
14	(13,600; 8850;-500)	(13,576; 8830;-500)	(-24;-20; 0)
15	(14,900; 9450;-500)	(14,894; 9452;-500)	(-6; 2;0)
16	(12,100; 7150;-500)	(12,113; 7141;-500)	(13;-9; 0)
17	(11,950; 8400;-500)	(11,968; 8422;-500)	(18; 22; 0)
18	(13,500; 7000;-500)	(13,519; 6982;-500)	(19;-18; 0)
19	(10,450; 7550;-500)	(10,463; 7570;-500)	(13; 20; 0)
20	(12,800; 7600;-500)	(12,823; 7584;-500)	(23;-16; 0)
21	(8700; 9450;-500)	(8687; 9443;-500)	(-13;-7; 0)
22	(9350; 8700;-500)	(9326; 8724;-500)	(-24; 24; 0)
23	(11,650; 9900;-500)	(11,656; 9920;-500)	(6; 20; 0)
24	(10,350; 9100;-500)	(10,349; 9089;-500)	(-1;-11; 0)
25	(14,350; 10,650;-500)	(14,365; 10,654;-500)	(15; 4;0)
26	(12,950; 11,550;-500)	(12,970; 11,541;-500)	(20;-9; 0)
27	(14,550; 10,900;-500)	(14,531; 10,919;-500)	(-19; 19; 0)
28	(14,000; 15,400;-500)	(13,981; 15,391;-500)	(-19;-9; 0)
29	(14,300; 13,150;-500)	(14,276; 13,169;-500)	(-24; 19; 0)
30	(12,800; 11,450;-500)	(12,814; 11,472;-500)	(14; 22; 0)
31	(14,650; 14,850;-500)	(14,650; 14,831;-500)	(0;-19; 0)

Case 2.1

Well Index	Drilling Site Position
1	(6200; 5700;-500)
2	(7050; 7200;-500)
3	(7100; 5600;-500)
4	(6200; 5700;-500)
5	(7100; 5600;-500)
6	(10,250; 6950;-500)
7	(9050; 5900;-500)
8	(9050; 5900;-500)
9	(3800; 4200;-500)
10	(3800; 4200;-500)
11	(7050; 7200;-500)
12	(5950; 7300;-500)
13	(13,900; 8600;-500)

(*continued on next page*)

(*continued*)

Well Index	Drilling Site Position
14	(13,900; 8600;-500)
15	(14,900; 9450;-500)
16	(12,050; 7750;-500)
17	(12,050; 7750;-500)
18	(13,200; 7250;-500)
19	(10,250; 6950;-500)
20	(13,200; 7250;-500)
21	(9050; 9050;-500)
22	(9050; 9050;-500)
23	(11,000; 9500;-500)
24	(11,000; 9500;-500)
25	(14,500; 10,850;-500)
26	(12,900; 11,500;-500)
27	(14,500; 10,850;-500)
28	(14,350; 15,100;-500)
29	(14,300; 13,150;-500)
30	(12,900; 11,500;-500)
31	(14,350; 15,100;-500)

Case 2.2

Well Index	Drilling Site Position
1	(6200; 5700;-500)
2	(7050; 7200;-500)
3	(7100; 5600;-500)
4	(6200; 5700;-500)
5	(7100; 5600;-500)
6	(10,100; 6300;-500)
7	(9050; 5900;-500)
8	(9050; 5900;-500)
9	(3700; 3550;-500)
10	(3900; 4850;-500)
11	(7050; 7200;-500)
12	(5950; 7300;-500)
13	(13,900; 8600;-500)
14	(13,900; 8600;-500)
15	(14,900; 9450;-500)
16	(12,450; 7350;-500)
17	(11,950; 8400;-500)
18	(13,500; 7000;-500)
19	(10,450; 7550;-500)
20	(12,450; 7350;-500)
21	(9050; 9050;-500)
22	(9050; 9050;-500)
23	(11,650; 9900;-500)
24	(10,350; 9100;-500)
25	(14,500; 10,850;-500)
26	(12,900; 11,500;-500)
27	(14,500; 10,850;-500)
28	(14,350; 15,100;-500)
29	(14,300; 13,150;-500)
30	(12,900; 11,500;-500)
31	(14,350; 15,100;-500)

Case 3.1

Well Index	Drilling Site Position
1	(6450; 5900;-500)
2	(6450; 5900;-500)
3	(6450; 5900;-500)
4	(6450; 5900;-500)
5	(8900; 5800;-500)
6	(8900; 5800;-500)
7	(8900; 5800;-500)
8	(8900; 5800;-500)
9	(3700; 3550;-500)
10	(3900; 4850;-500)
11	(6950; 7750;-500)
12	(5950; 7300;-500)

(*continued on next page*)

(*continued*)

Well Index	Drilling Site Position
13	(14,250; 8350;-500)
14	(13,600; 8850;-500)
15	(14,900; 9450;-500)
16	(12,600; 7500;-500)
17	(12,600; 7500;-500)
18	(12,600; 7500;-500)
19	(9750; 8650;-500)
20	(12,600; 7500;-500)
21	(9750; 8650;-500)
22	(9750; 8650;-500)
23	(11,650; 9900;-500)
24	(9750; 8650;-500)
25	(14,000; 11,050;-500)
26	(14,000; 11,050;-500)
27	(14,000; 11,050;-500)
28	(14,000; 15,400;-500)
29	(14,300; 13,150;-500)
30	(14,000; 11,050;-500)
31	(14,650; 14,850;-500)

Case 3.2

Well Index	Drilling Site Position
1	(5550; 5350;-500)
2	(6750; 5850;-500)
3	(6750; 5850;-500)
4	(6750; 5850;-500)
5	(6750; 5850;-500)
6	(10,250; 6950;-500)
7	(9050; 5900;-500)
8	(9050; 5900;-500)
9	(3800; 4200;-500)
10	(3800; 4200;-500)
11	(6450; 7550;-500)
12	(6450; 7550;-500)
13	(13,900; 8600;-500)
14	(13,900; 8600;-500)
15	(14,900; 9450;-500)
16	(12,600; 7500;-500)
17	(12,600; 7500;-500)
18	(12,600; 7500;-500)
19	(10,250; 6950;-500)
20	(12,600; 7500;-500)
21	(9050; 9050;-500)
22	(9050; 9050;-500)
23	(11,000; 9500;-500)
24	(11,000; 9500;-500)
25	(14,500; 10,850;-500)
26	(12,900; 11,500;-500)
27	(14,500; 10,850;-500)
28	(14,350; 15,100;-500)
29	(14,300; 13,150;-500)
30	(12,900; 11,500;-500)
31	(14,350; 15,100;-500)

Case 3.3

Well Index	Drilling Site Position		Difference
	Grid Value	Accurate Value	
1	(6200; 5700;-500)	(6183; 5702;-500)	(-17; 2;0)
2	(7050; 7200;-500)	(7037; 7211;-500)	(-13; 11; 0)
3	(7100; 5600;-500)	(7122; 5594;-500)	(22;-6; 0)
4	(6200; 5700;-500)	(6183; 5702;-500)	(-17; 2;0)
5	(7100; 5600;-500)	(7122; 5594;-500)	(22;-6; 0)
6	(10,100; 6300;-500)	(10,111; 6284;-500)	(11;-16; 0)
7	(9050; 5900;-500)	(9025; 5890;-500)	(-25;-10; 0)
8	(9050; 5900;-500)	(9025; 5890;-500)	(-25;-10; 0)
9	(3700; 3550;-500)	(3689; 3571;-500)	(-11; 21; 0)

(*continued on next page*)

(*continued*)

Well Index	Drilling Site Position		Difference
	Grid Value	Accurate Value	
10	(3900; 4850;-500)	(3917; 4849;-500)	(17;-1; 0)
11	(7050; 7200;-500)	(7037; 7211;-500)	(-13; 11; 0)
12	(5950; 7300;-500)	(5956; 7304;-500)	(6; 4;0)
13	(13,900; 8600;-500)	(13,892; 8604;-500)	(-8; 4;0)
14	(13,900; 8600;-500)	(13,892; 8604;-500)	(-8; 4;0)
15	(14,900; 9450;-500)	(14,894; 9452;-500)	(-6; 2;0)
16	(12,450; 7350;-500)	(12,470; 7347;-500)	(20;-3; 0)
17	(11,950; 8400;-500)	(11,968; 8422;-500)	(18; 22; 0)
18	(13,500; 7000;-500)	(13,519; 6982;-500)	(19;-18; 0)
19	(10,450; 7550;-500)	(10,463; 7570;-500)	(13; 20; 0)
20	(12,450; 7350;-500)	(12,470; 7347;-500)	(20;-3; 0)
21	(9050; 9050;-500)	(9025; 9052;-500)	(-25; 2;0)
22	(9050; 9050;-500)	(9025; 9052;-500)	(-25; 2;0)
23	(11,650; 9900;-500)	(11,656; 9920;-500)	(6; 20; 0)
24	(10,350; 9100;-500)	(10,349; 9089;-500)	(-1;-11; 0)
25	(14,500; 10,850;-500)	(14,482; 10,858;-500)	(-18; 8;0)
26	(12,900; 11,500;-500)	(12,893; 11,505;-500)	(-7; 5;0)
27	(14,500; 10,850;-500)	(14,482; 10,858;-500)	(-18; 8;0)
28	(14,350; 15,100;-500)	(14,329; 15,104;-500)	(-21; 4;0)
29	(14,300; 13,150;-500)	(14,276; 13,169;-500)	(-24; 19; 0)
30	(12,900; 11,500;-500)	(12,893; 11,505;-500)	(-7; 5;0)
31	(14,350; 15,100;-500)	(14,329; 15,104;-500)	(-21; 4;0)

Case 4

Well Index	Drilling Site Position
1	(6500; 5650;-500)
2	(6700; 7250;-500)
3	(6500; 5650;-500)
4	(6500; 5650;-500)
5	(6500; 5650;-500)
6	(10,250; 6950;-500)
7	(9050; 5900;-500)
8	(9050; 5900;-500)
9	(3800; 4200;-500)
10	(3800; 4200;-500)
11	(6700; 7250;-500)
12	(6700; 7250;-500)
13	(14,200; 8900;-500)
14	(14,200; 8900;-500)
15	(14,200; 8900;-500)
16	(12,850; 7200;-500)
17	(11,800; 9150;-500)
18	(12,850; 7200;-500)
19	(10,250; 6950;-500)
20	(12,850; 7200;-500)
21	(9500; 9050;-500)
22	(9500; 9050;-500)
23	(11,800; 9150;-500)
24	(9500; 9050;-500)
25	(14,500; 10,850;-500)
26	(12,900; 11,500;-500)
27	(14,500; 10,850;-500)
28	(14,350; 15,100;-500)
29	(14,300; 13,150;-500)
30	(12,900; 11,500;-500)
31	(14,350; 15,100;-500)

References

Devine, M., Lesso, W., 1972. Models for the minimum cost development of offshore oil fields. Manag. Sci. 18 pp. B-378-B-387.

Dogru, S., 1987. Selection of optimal platform locations. SPE Drill. Eng. 2, 382–386, 1987/12/1/.

Frair, L., Devine, M., 1975. Economic optimization of offshore petroleum development. Manag. Sci. 21, 1370–1379.

Garcia-Diaz, J.C., Startzman, R., Hogg, G.L., 1996. A new methodology for minimizing investment in the development of offshore fields. SPE Prod. Facil. 11, 22–29, 1996/2/1/.

Goel, V., Grossmann, I.E., 2004. A stochastic programming approach to planning of offshore gas field developments under uncertainty in reserves. Comput. Chem. Eng. 28, 1409–1429, 2004/07/15/.

Hansen, P., de Luna Pedrosa Filho, E., Carneiro Ribeiro, C., 1992. Location and sizing of offshore platforms for oil exploration. Eur. J. Oper. Res. 58, 202–214, 1992/04/27/.

Iyer, R.R., Grossmann, I.E., Vasantharajan, S., Cullick, A.S., 1998. Optimal planning and scheduling of offshore oil field infrastructure investment and operations. Ind. Eng. Chem. Res. 37, 1380–1397, 1998/04/01.

Lillevik, E., Standal, I.E., 2018. The Traveling Circus - Automated Generation of Parametric Wellbore Trajectories Minimizing Wellbore Lengths for Different Subsea Field Layouts. Master. Department of Geoscience and Petroleum, Norwegian University of Science and Technology.

Tavallali, M.S., Karimi, I.A., Halim, A., Baxendale, D., Teo, K.M., 2014. Well placement, infrastructure design, facility allocation, and production planning in multireservoir oil fields with surface facility networks. Ind. Eng. Chem. Res. 53, 11033–11049, 2014/07/09.

Wang, Y., Estefen, S.F., Lourenço, M.I., Hong, C., 2019. Optimal design and scheduling for offshore oil-field development. Comput. Chem. Eng. 123, 300–316, 2019/04/06/.